Earth and Planetary Science Letters 297 (2010) 471–480

Contents lists available at ScienceDirect

Earth and Planetary Science Letters

journal homepage: www.elsevier.com/locate/epsl

Rheology and flow of crystal-bearing lavas: Insights from analogue gravity currents

Angelo Castruccio [a,b,*], A.C. Rust [a], R.S.J. Sparks [a]

[a] Department of Earth Sciences, University of Bristol, Wills Memorial Building, Queen's Road, Bristol BS8 1RJ, United Kingdom
[b] Departamento de Geología, Universidad de Chile, Plaza Ercilla 803, Casilla 13518, Santiago, Chile

ARTICLE INFO

Article history:
Received 11 December 2009
Received in revised form 28 June 2010
Accepted 30 June 2010
Available online 31 July 2010

Editor: L. Stixrude

Keywords:
rheology
suspensions
yield strength
lava flow
2-D simulation

ABSTRACT

The rheology of suspensions of cubic crystals in viscous liquids was investigated with a series of experiments, consisting of the release of a fixed volume of fluid inside a horizontal channel. A Herschel–Bulkley rheology was assumed and the consistency K and the shear rate exponent n of this constitutive equation were calculated using the evolution of the flow front; the yield strength was calculated using the final shape of the flow. A solid fraction by volume of $\phi = 0$–0.67 and a liquid viscosity range of 1–370 Pa s were used in the experiments. Results show an increase in K when crystal content increases. The mixtures start to show a shear thinning behaviour at $\phi \sim 0.3$ with n values going from approximately 1 (Newtonian behaviour) to 0.5 at $\phi = 0.6$. Yield strength was detected at the same ϕ as the beginning of shear thinning behaviour and increases with a power-law relationship with crystal content. Suspensions with bimodal size distribution of crystals show a dramatic decrease of the apparent viscosity compared to unimodal suspensions, especially at the higher total crystal concentrations. The results were applied to theoretical 2-D flows on a slope, showing large variations in velocity profiles for the same crystallinity depending on the rheology assumed. A case study of a 2002 lava flow from Etna volcano demonstrates that measured lava flow speeds are similar to speeds calculated from 2-D theory with rheologies of lava based on laboratory experiments and measured lava crystal content. The results illustrate that the dynamics of lava flows depend on the crystal size distribution in addition to the total crystal concentration.

1. Introduction

An understanding of the rheology of magma is of importance in the study of a number of geological issues, such as the ascent and emplacement of magmas in the continental crust (Petford, 2003), magma ascent dynamics inside a volcanic conduit (Melnik and Sparks, 1999; Papale, 2001) and the emplacement of lavas (e.g. Huppert, 1982a,b; Dragoni et al., 1986, 2005; Kerr and Lyman, 2007). Magma rheology is also important for the forecasting of eruptions (Dingwell, 1996; Sparks, 2003). The main factors that affect the rheology of magma are: the degree of polymerisation of the melt, which is directly related to its chemical composition and temperature; the content, shape and size distribution of crystals; and the content and size of bubbles.

Lava flows are the most easily observed magma flows and provide an opportunity to validate rheological models of magmas. Some early models of lava flows used a Newtonian rheology (e.g. Huppert et al., 1982; Takagi and Huppert, in press) to describe the evolution of lava flows and domes, but the most widely used rheology has been the Bingham model, which is characterized by a yield strength and a plastic viscosity (e.g. Hulme, 1974; Dragoni et al., 1986; Ishihara et al., 1990; Harris and Rowland, 2001). Despite numerous works mentioning the existence of a non-linear relationship between shear rate and stress in crystal-bearing lavas (e.g. McBirney and Murase, 1984; Pinkerton and Norton, 1995; Lavallée et al., 2007), there is little work regarding the dynamics of flows with a non-linear rheology (e.g. Balmforth and Craster, 2000) and their application to lava flows.

In this study, we have chosen a different approach in order to investigate the rheology of crystal-bearing magmas. We carried out analogue experiments that involved the sudden release of a fixed volume of a suspension inside a horizontal channel. This kind of system is sometimes described as a dam break, and has been used before to study the dynamics of Newtonian fluids on a slope (Huppert, 1982b), to determine the rheology of foods (Bostwick consistometer, Balmforth et al., 2007) and also to study the dynamics of analogue lava flows with fluids of known rheology (Lyman et al., 2005; Lyman and Kerr, 2006). Here we use the evolution of dam break flows, to infer the rheology of suspensions in a viscous liquid.

We used sugar syrup (Tate & Lyle) as the liquid phase and sugar crystals as the solid, noting that this system provides a good analogy of phenocrysts suspended in a silicate melt. Numerous authors have used syrup alone or with suspended crystals as analogue materials to study the dynamics (Stasiuk et al., 1993) or the rheology (Hoover et al., 2001; Soule and Cashman, 2005) of lava flows. Here, we investigated the influence of the crystal content and grain size

* Corresponding author. Department of Earth Sciences, University of Bristol, Wills Memorial Building, Queen's Road, Bristol BS8 1RJ, United Kingdom. Tel.: +44 117 9706156; fax: +44 117 9253385.
E-mail address: angelo.castruccio@bristol.ac.uk (A. Castruccio).

0012-821X/$ – see front matter © 2010 Elsevier B.V. All rights reserved.
doi:10.1016/j.epsl.2010.06.051

distribution on the rheology of suspensions and compare the results with previous studies. In order to investigate the rheological properties we measured the flow front evolution and the final shape of the flow. We used the mathematical framework of Balmforth et al. (2007) to interpret the data, adopting the Herschel–Bulkley rheological model. We discuss the advantages of this method for the study of the rheology of suspensions compared with others, such as rotational rheometer measurements. Finally, we consider the implications of our results for the rheology of lava flows, using a simplified 2-D model to investigate the effects of different rheological models of suspensions on the flow of lava. We validated our results using data from lava flows of the 2002 Etna volcano eruption.

2. Rheological models for suspensions

Einstein (1906) found that for a very dilute suspension of spheres, the relative viscosity can be calculated as:

$$\mu_r = (1 + B_s\phi), \tag{1}$$

where μ_r is the relative viscosity (the ratio between the viscosity of the suspension and the viscosity of the suspending liquid), ϕ is the volume concentration of particles and B_s is a constant with a value of 2.5 for spheres. Roscoe (1952) extended the relationship to higher concentrations of spheres in the form of

$$\mu_r = \left(1-\frac{\phi}{\phi_m}\right)^{-2.5}, \tag{2}$$

where ϕ_m is the maximum packing fraction (i.e. the maximum concentration that can be attained by the solids). A generalized form of Eq. (2) was given by Krieger and Dougherty (1959):

$$\mu_r = \left(1-\frac{\phi}{\phi_m}\right)^{-B_e\phi_m}, \tag{3}$$

where B_e is a constant sometimes called the "Einstein coefficient" (Costa, 2005). The last two equations converge to the Einstein relationship (Eq. (1)) for low concentrations and asymptote to infinite viscosity when ϕ approaches ϕ_m.

The Einstein–Roscoe formulation (Eq. (2)) has been widely used for volcanological and petrological applications. For example, Shaw (1969) used it to explain the changes in viscosity due to crystal content of basalts. Marsh (1981) applied the formula for the calculation of viscosities of magmas, using a value of 0.6 for ϕ_m. Pinkerton and Stevenson (1992) used the equation for lavas with low crystals contents. Lejeune and Richet (1995) noted that their laboratory measurements of viscosity of silicate melts with suspended crystals agree with the Eq. (2) for crystal concentrations up to about 40% by volume. Many others studies have used the equation for mathematical modelling of magma chamber or conduit flow dynamics. (e.g. Huppert and Sparks, 1988; Papale et al., 1998).

Although widely applied, a limitation of the rheological relationships discussed above (Eq. (1)–(3)) is that they do not take into account the onset of non-Newtonian effects such as yield strength and strain rate-dependent viscosity, which may be significant at high crystal (or bubble) concentrations (Pinkerton and Norton, 1995; Costa et al., 2009). Furthermore, these constitutive equations do not consider the effects of polymodal size distributions of particles of porphyritic magmas.

2.1. Non-Newtonian rheology

Although silicate melts are Newtonian for a range of shear rates (Costa et al., 2009), many studies suggest that with sufficient crystals, magmas become non-Newtonian. Most studies of the rheology of magmas have identified a shear thinning behaviour (decrease in the viscosity with higher strain rates) with increasing crystal concentration. Pinkerton and Stevenson (1992) presented empirical formulae for different strain rate ranges, showing that, for low strain rates, Eq. (2) is still valid for laboratory experiments on lavas of a range of compositions. Pinkerton and Norton (1995) found that Etna lavas showed a shear thinning behaviour with a decrease in temperature and increase in crystal concentration, with n decreasing from 1 to 0.46. Lavallée et al. (2007) found that the rheology of several samples of high crystalline lavas (crystal volume fraction of 0.5–0.8) determined in the laboratory fit a power law equation with $n = 0.51$. Costa et al. (2009) presented an empirical relationship that incorporated the effects of strain rate on the viscosity of suspensions.

Yield strength, which is the stress below-which there is effectively no flow, is another potential non-Newtonian property of crystal-rich magmas. Robson (1967) proposed that crystal-rich lavas possess a yield strength, based on the data of Walker (1967) on the thickness of lavas on Etna volcano, suggesting a maximum yield strength of about 2.2×10^4 Pa. Hulme (1974) attributed the formation of levées on lava flows to yield strength and developed a theoretical formulation to estimate the yield strength using the final dimensions of the lava. Sparks et al. (1976) reported values of yield strength in the range of 10^2–10^3 Pa for Etnean lavas using the Hulme theory. Petford and Koenders (1998) summarized the values of yield strength obtained for lavas in different studies with a range of 10^2–10^6 Pa for different compositions and crystallinities.

The parameterization of the factors involved in controlling yield strength has proved to be a difficult task and is still far from being resolved. Hulme (1974) suggested a linear relationship between yield strength and overall silica content, but, as pointed out by McBirney and Murase (1984), without taking into consideration the effects of temperature or crystal content. Diverse formulas of yield strength versus ϕ have been given by different authors (e.g. Gay et al., 1969; Ryerson et al., 1988; Dragoni and Tallarico, 1994; Zhou et al., 1995), but the computed values can be very different (see Fig. 6 in Section 4.3).

Kerr and Lister (1991) argued that yield strength can develop only when a touching framework of crystals forms, so that only mixtures with crystal concentration higher than about 50% for spherical mixtures can show a yield strength. They also mentioned that if the crystals are elongated they can connect at much lower values of ϕ. They suggested that the yield strengths reported by others authors could be due to artefacts due to the extrapolation of the rheological curve (stress vs strain rate) to zero stress. Saar et al. (2001) showed with computer simulations that crystal networks can be formed at ϕ as low as ~0.2, depending on the crystal shape and shear rate. Barnes (1999) reviewed the concept of yield strength in general and postulated that it does not exist, in the sense that there is no stress limit under which there is no deformation, instead there is a huge increase in the viscosity close to zero stress. However, Barnes (1999) also pointed out that the concept of yield strength has practical value if the stress and strain rate ranges are clearly specified. Lavallée et al. (2007) and Caricchi et al. (2007) reported no yield strength for highly crystalline lavas (50–80% by volume). However, the very high (~10^6 Pa) applied pressures would not enable yield strengths <10^6 Pa to be detected, and most estimates from lava flow and dome morphologies are considerably lower than this (Petford and Koenders, 1998; Lyman et al., 2004).

2.2. Polymodal suspensions

Many magmas have polymodal size-distributions of crystals, which could affect rheology as a function of crystal content because small crystals may be able to pass through gaps between larger crystals. In equations such as Eqs. (2) and (3) it has long been recognized that crystal size distribution and shape are likely to affect

the value of ϕ_m (e.g. Mcbirney and Murase, 1984). Chong et al. (1971) performed experiments with bimodal suspensions, showing a strong dependence of viscosity on the fine particle content and the ratio between the sizes of the particles. Chang and Powell (1993, 1994) made numerical simulations and laboratory measurements with bimodal suspensions, showing that the lowest values for viscosity (and consequently the highest values of ϕ_m) are reached for a fine content of near 0.25 and a size ratio between small and large particles of 10:1.

2.3. Rheological model used

In this study we characterize the rheology of the suspensions with Herschel and Bulkley (1926) model,

$$\tau = \tau_y + K\dot{\gamma}^n, \tag{4}$$

where τ is the applied stress, $\dot{\gamma}$ is the strain rate, n is a flow index, K is the consistency and is a measure of effective viscosity and τ_y is the yield strength. This equation takes into account changes in viscosity ($\tau/\dot{\gamma}$) with strain rate. It reduces to the Newtonian case when $\tau_y = 0$ and $n = 1$, and to the Bingham model when $n = 1$ and $\tau_y > 0$. If $n > 1$ the fluid rheology is shear thickening, and if $n < 1$ it is shear thinning.

3. Theoretical background of 2D gravity currents

Here, we present the method and mathematical background elaborated by Balmforth et al. (2007) used to determine the fluids rheology from dam break flows. The experimental setup consisted of a horizontal channel where the studied fluid is held, with an initial length L and height H, behind a removable wall (Fig. 1a). Once the wall is lifted, the position of the front of the flow against time is recorded.

We assumed a rheology in the form of Eq. (4). The evolution of the length of the flow is of the form

$$x = C{*}t^b, \tag{5}$$

where x is the front position at time t. The value of the constant C is then used to determine the parameter K in Eq. (4), while the exponent b depends on the exponent n in Eq. (4). Finally, the yield strength is obtained using the final shape of the flow, that is, the final height as a function of x.

For dam breaks, three regimes can be recognized through theoretical analysis. At the beginning the flow is dominated by inertia and the velocity is proportional to $\sqrt{gH}$ and consequently $x \propto t$. After a transition time (when $t \sim H^2/\mu_k$ for the Newtonian case, where μ_k is the kinematic viscosity and it is viscosity/density) the viscous forces become the dominant retarding force and the front position is in the form $x \propto t^{n/(n+1)}$. For the long time regime, there is the additional condition that the product length*height of the flow can be approximated as a constant and the front evolution is in the form $x \propto t^{n/(2n+3)}$. For the Newtonian case the relationships reduce to $x \propto t^{1/2}$ for short times and $x \propto t^{1/5}$ for long times (Balmforth et al., 2007).

The yield strength and surface tension effects are assumed to be small enough to be neglected at the start of the experiments. Surface tension begins to be important only when the flow is very thin (a couple of mm), and yield strength affects the evolution of the flow when it has slowed down enough, so that $\tau_y \sim K\dot{\gamma}^n$. It can be shown that the equation for the front position for a fluid inside a channel in the short time regime can be written as:

$$x(t) = AH^{\frac{n+2}{n+1}}\left(\rho\frac{g}{K}\right)^{\frac{1}{n+1}}t^{\frac{n}{n+1}}, \tag{6}$$

where A is a constant, ρ is density and g is gravity. For the Newtonian case this reduces to:

$$x(t) = A_n H^{\frac{3}{2}}\sqrt{\frac{\rho g}{\mu}}t^{1/2}, \tag{7}$$

where μ is the viscosity and $A_n = 0.2845$. In this way, n can be deduced from the time exponent and K can be extracted if the constant A is known.

For short times, A is a function of n in Eq. (6). Some values of A as function of n were calculated from 2D numerical simulations carried out by Balmforth et al. (2007) without considering side walls, and it can be approximated by:

$$A = 0.0594\ln(n) + A_n. \tag{8}$$

To calculate the yield strength, Balmforth et al. (2007) applied a scaled yield strength or Bingham number,

$$B = \frac{\tau_y L}{\rho g H^2}. \tag{9}$$

Using mathematical analysis they arrived to the following relationship for infinite times (final profile of the flow):

$$h_\infty = \sqrt{(3B)^{2/3} - 2Bx} \qquad \text{if } B < 1/3, \tag{10}$$

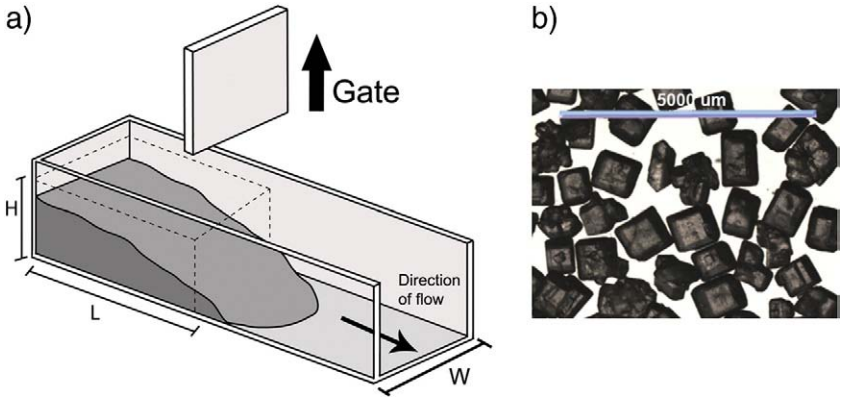

Fig. 1. a) Experimental setup. H and L are the initial height and length of the fluid inside the channel before the release of the gate. b) Microscopic picture of sugar particles used in the experiments.

for full slumps or

$$h_\infty = \begin{cases} \sqrt{\left(\frac{6B + 1 - 6Bx}{3}\right)} & 1-(3B)^{-1} \le x \le 1 + (6B)^{-1} \\ 1 & 0 < x < 1-(3B)^{-1} \end{cases} \quad \text{if } B > 1/3, \tag{11}$$

for partial slumps, where h_∞ is the final height of the flow at a given position. Therefore, knowing the final length (where $h=0$) and profile of the flow, the B number (and consequently, the yield strength) can be calculated.

Additional axisymmetric experiments were performed to measure the yield strength, in a geometry unaffected by sidewalls. These experiments consisted in the release of a fixed volume of the mixture in a flat surface. The final radius R and maximum height H were measured in order to calculate the yield strength using the following formula (Nye, 1952):

$$\tau_y = 0.5 g \rho \frac{R^2}{H}. \tag{12}$$

4. Experiments

4.1. Materials used

The dam break experiments were carried out in a perspex channel, 5 cm wide, 10 cm in height and 80 cm long. A fixed volume of liquid with suspended crystals is contained within the channel behind a gate. The gate is then lifted and the material is allowed to flow horizontally. The evolution of the front flow is recorded with a video camera. The suspending fluid consisted of golden syrup (Tate & Lyle) with a density of 1386 kg/m^3, which in some experiments was diluted by 5 or 10% by weight of water. The viscosity of the syrup was measured using a Haake V5 rotational rheometer and is strongly dependant on temperature, with an approximate viscosity of 78 Pa s at 20 °C. Temperature was measured for each experiment to account for its effect on viscosity.

The particles consisted of crystals of white sugar with a density of 1586 kg/m^3. The particles were sieved in the range 0.5–1 mm for most of the experiments (Fig. 1b), except the bimodal grain size population experiments, where particles in the range of 0.1–0.2 mm and 1–1.5 mm were used. The shape of the particles is approximately cubic, with a length–width ratio range between 1 and 2, with a mean value close to 1. The volume concentration of crystals ranged from 0 to 0.67.

Examination of the mixtures under a microscope established that there were no observable changes in shapes or size or number of crystals over periods of up to 2½ days, much longer than the scale of time of the experiments (~1 h).

4.2. Calibration

In this study we use the short time solution (Eq. (6)) because it is the only regime that can be identified clearly over the time scale of the experiments. A first series of experiments was carried out with different Newtonian fluids inside a channel 5 cm wide, with a known viscosity measured with a rotational rheometer, in order to find the value of A. The data collapse onto a single curve when length and time are plotted in non-dimensional forms (Balmforth et al., 2007) as X' and T' as:

$$X' = \frac{x}{L}, \tag{13}$$

$$T' = \frac{t}{T^*}, \text{where } T^* = \frac{L}{H}\left(\frac{KL}{\rho g H^2}\right)^{\frac{1}{n}}. \tag{14}$$

The slope of the curve is the value of the constant A and a value of $A=0.225$ was found (Fig. 2). This is slightly less than the value of A_n for 2D Newtonian flow, due to the retarding effects of sidewalls in the experiments. The time range (or an equivalent distance range) over which the calculations were done, was chosen based in Balmforth et al. (2007). Their data show that the short time solution is valid until around a dimensionless time of 4. The theoretical transition time between the inertia dominated regime and the short time regime is H^2/μ_k but was chosen specifically for each experiment based in the initial conditions such as initial height, crystal concentration and liquid viscosity, as in our experiments the inertia regime appears to dominate for some time after the theoretical time value.

Another series of experiments were carried out to determine the dependence of A on channel width, using golden syrup and xanthan gum and widths from 2.5 to 19 cm. A simple way to model the relationship is assuming that the constant A depends on the wall effects and can be described as the wetted perimeter per unit area:

$$WC/(W + 2C), \tag{15}$$

where W is the channel width and C is a constant to be determined by fitting the experiments data with Newtonian flows. Normalizing by 0.2845, for large W, the experiments give a very good fit (within a 5% of the expected values, for widths greater than 2.5 cm) to Eq. (15). Thus, using Eq. (8), the value of A can be described by an empirical function of channel width, W (cm), and exponent n of the fluid in the form:

$$A = \left[\frac{W}{W + \frac{1.2}{n}}\right](0.0594 \ln(n) + A_n), \tag{16}$$

With W and the constant 1.2 in cm. While Eq. (16) works for fluids with n between 1 and 0.2 in channels with a width between 2.5 and 19 cm, it has yet to be verified beyond conditions of our experiments.

Analysis of fluid properties from rheometer data generally assume that there is no slip near fluid–wall interfaces. According to Barnes (1995) slip occurs due to the displacement of particles away from the wall boundaries in two phase systems, mainly because of hydrodynamic and viscoelastic forces in a very thin layer. A common technique to minimize this effect is to use a rough wall, ideally made with the same type of particles as the suspension. A rough base, made of cardboard with crystals glued to it, was put in the channel to test these effects in our experiments. For syrup up to $\phi=0.27$, the rough base has little effect and the calculated n and K are within error margins (Fig. 3). In contrast, for syrup with $\phi=0.47$ and 0.55 the

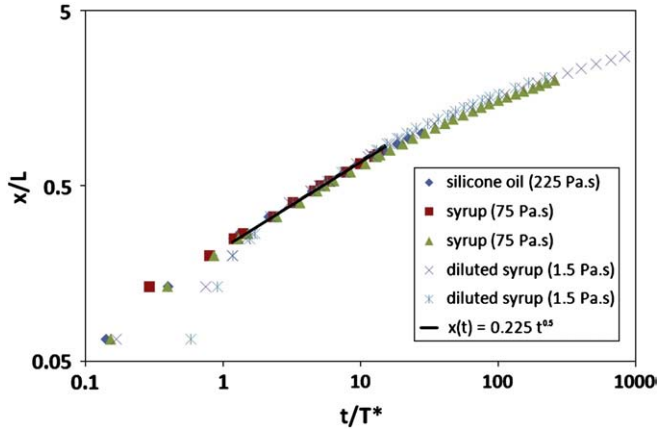

Fig. 2. Dimensionless distance versus time for different experiments using Newtonian fluids with viscosities of 1, 75 and 225 Pa s. The data collapse for a value of $A=0.225$ for short time solutions.

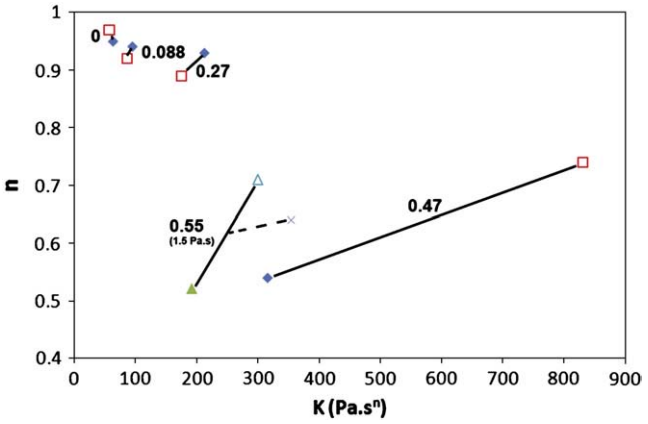

Fig. 3. Values of n and K of Eq. (4) found in the experiments using rough and smooth bases. Diamonds are values using a rough base. Open squares are values using a smooth base. Triangles are experiments using diluted syrup (1.5 Pa s). Filled triangle is a rough base experiment and open triangle is with a smooth base. Also plotted is the measurement with a rotational rheometer. Numbers indicate the solid concentration of the experiments.

differences are noticeable (40% to 250% in the values of n and K). The experimental results also show that the rotational rheometer measurements done on suspensions with high crystal content are closer to experiments with a smooth base, suggesting that these measurements were also affected by wall slip. With the exception of Fig. (3), all data presented in figures or tables were collected with a rough base.

4.3. Results

The calculated values for the parameters K, n and τ_y of the Herschel–Bulkley model (Eq. (4)) for experiments with unimodal size distribution are plotted in Figs. 4–6. The parameters used in the experiments are specified in Table 2S (Supplementary material). Table 3S (Supplementary material) shows additional experiments done to calculate the yield strength using different setups (axysimmetric) and conditions (different liquid viscosities).

The consistency K increases as the particle concentration ϕ increases (Fig. 4). The trends are different depending on the water concentration of the syrup (Fig. 4a). In Fig. 4b, the consistency has been normalized by the suspending liquid viscosity (K_0). It should be noted that the dimensions of K depend on n, which in turn depends on ϕ. The data are well fitted by using a modified version of the Einstein–Roscoe Eq. (17), using consistency instead of viscosity.

The value of n remains close to 1 until about $\phi = 0.27$, above which it starts to decrease to 0.5 at $\phi = 0.56$ (Fig. 5).

In Fig. 6 the relationship between yield strength and particle concentration is plotted. The calculated values are similar for different liquid viscosities used; except for liquid viscosities of 1.5 Pa s which are at least 1 order of magnitude lower as discussed in the next section. The best fitting of the data is given by a power law fit in the form of Eq. (18). Different relationships between yield strength and crystal concentration proposed by several authors are also plotted in Fig. 6. Of these, the formulation of Zhou et al. (1995) fits our data best, but it does not fit well values above $\phi = 0.53$.

In summary, we have obtained the following parameterization of the values of K, n and τ_y of the Herschel–Bulkley equation as a function of particle concentration ϕ:

$$K(\phi) = K_0\left(1-\frac{\phi}{\phi_m}\right)^{-2.3}, \tag{17}$$

$$\tau_y(\phi) = \begin{cases} 0 & \phi \le \phi_c \\ D(\phi-\phi_c)^8 & \phi > \phi_c \end{cases}, \tag{18}$$

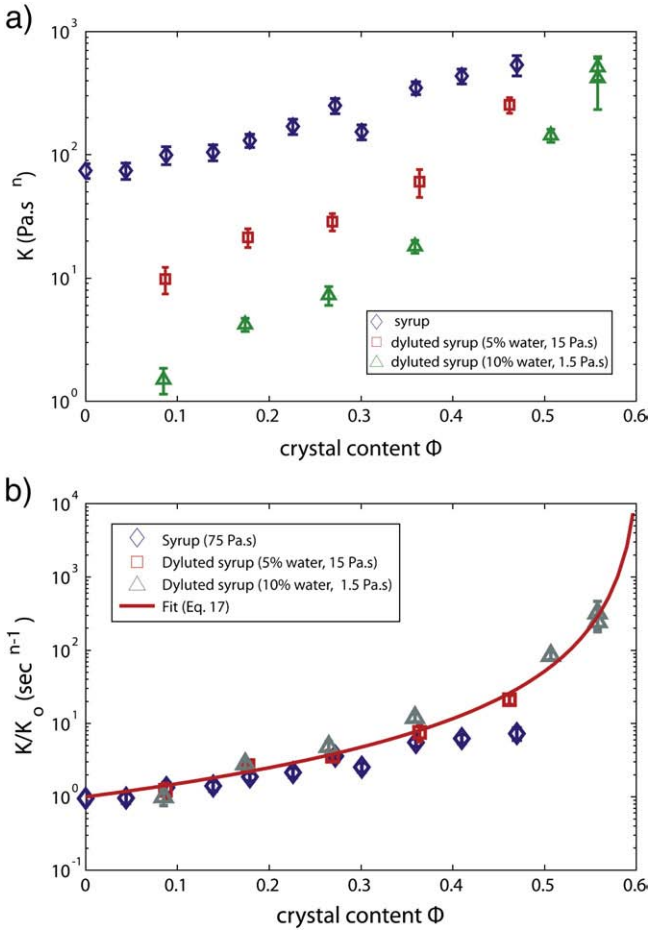

Fig. 4. a) Calculated K versus crystal content for different liquid viscosities. b) K normalized by the initial viscosity raised to n (note that K has varying dimensions). The fit is given by a modified Einstein–Roscoe equation (Eq. 17).

$$n(\phi) = \begin{cases} 1 & \phi \le \phi_c \\ 1 + 1.3\left(\frac{\phi_c-\phi}{\phi_m}\right) & \phi > \phi_c \end{cases}, \tag{19}$$

where ϕ_c is the particle concentration when shear thinning appears ($\phi_c = 0.27$), and was obtained from Fig. 5. $\phi_m = 0.6$ was obtained by fitting the apparent viscosity of the mixtures with different particle

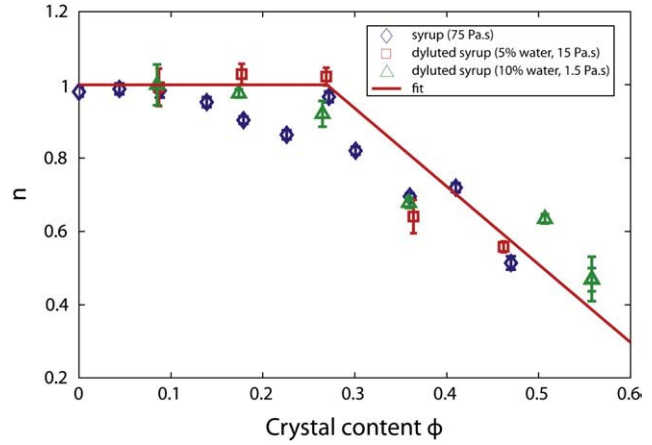

Fig. 5. Calculated n versus crystal content for different liquid viscosities. The line is the plot of Eq. (19).

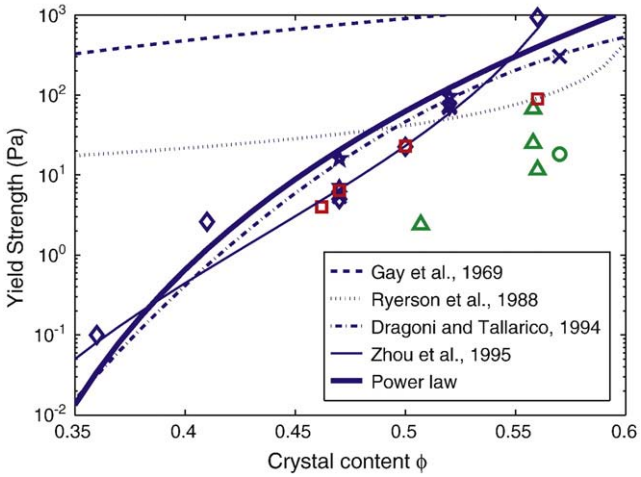

Fig. 6. Calculated yield strength versus crystal concentrations. The relationships given by different authors and a power law relationship (Eq. (18)) are also plotted. Diamond = syrup (75 Pa s); square = diluted syrup (5% water 15 Pa s); triangle = diluted syrup (10% water, 1.5 Pa s); five-point star = syrup (10 °C, 370 Pa s); six-point star = syrup (axisymmetric, 75 Pa s); × = syrup (axisimmetric, 10 °C, 370 Pa s); circle = diluted syrup (axisimmetric, 10% water, 1.5 Pa s).

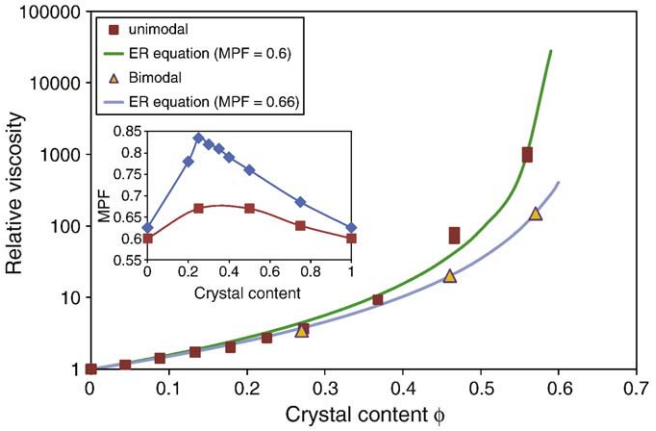

Fig. 8. Relative viscosity versus crystal content. The unimodal experiments can be fitted with the Einstein–Roscoe equation, using a value of $\phi_m = 0.6$. The bimodal experiments (50% fine by volume) also can be fitted with the Einstein–Roscoe equation, but with a value of $\phi_m = 0.66$. The inset box shows the maximum packing fraction versus fine content, calculated by fitting the apparent viscosity with the Einstein–Roscoe equation (filled squares). For comparison, data from Sudduth (1993) for spherical particles are also presented (filled diamonds).

concentrations with the Einstein–Roscoe equation. D is a constant with a value of 5×10^6 Pa.

The results of the experiments with a bimodal crystal size distribution are plotted in Fig. 7. The parameters used in the experiments are in Table 4S (Supplementary material). Two end members were used: fine crystals (sieved to 0.2–0.5 or 0.1–0.2 mm) and coarse crystals (1.5 mm). The experiments were carried out at three different total concentrations: 0.27, 0.47 and 0.56. For low concentrations ($\phi = 0.27$) the effect of the size distribution on the apparent relative viscosity (defined as the viscosity at the strain rate of the experiment with respect to the liquid viscosity) is small and the values obtained for different size distributions are similar. For higher concentrations ($\phi = 0.47$) the effects are noticeable and more marked when the size ratio between particles is higher. The apparent relative viscosity reaches a minimum when the size distribution is 50% of fine particles. For concentrations of $\phi = 0.56$ the difference in the apparent relative viscosity is more than an order of magnitude between unimodal (100% of fine or coarse particles) and bimodal (50% of fines) distributions. As discussed in Section **5**, the results can be approximately described with effective medium theory assuming that the "fluid phase" is made of syrup plus the fine crystals and the solid phase by the coarse crystals (plotted lines in Fig. 7) or, alternatively, using different values for ϕ_m in the Einstein–Roscoe equation (Fig. 8).

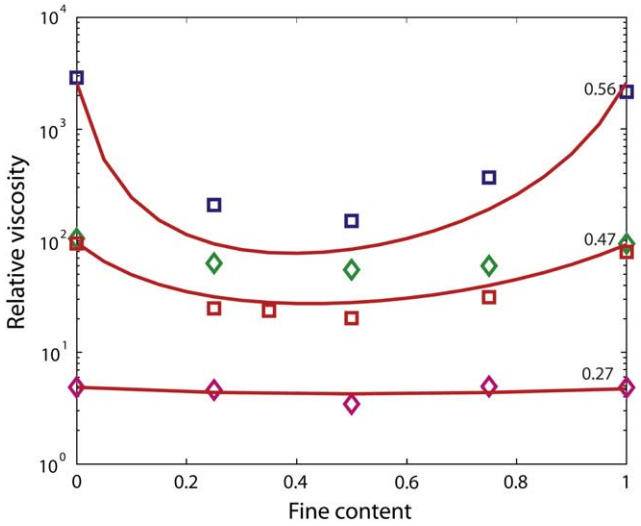

Fig. 7. Relative viscosity for different particle size distributions between two populations (fine and coarse). Numbers indicate total crystal content. Diamonds are experiments with a size ratio of particles of 5:1. Squares are experiments with a size ratio of 10:1. The curves show the calculated variation of viscosity using the Einstein–Roscoe equation, assuming the effective fluid phase is the syrup + fine crystals and the particles are the coarse crystals.

Fig. 8 is a plot of the apparent Newtonian viscosity versus the crystal content. For the experiments with a non-Newtonian rheology, the apparent viscosity was calculated with the best fit of the experimental data (front position vs time) with a "Newtonian" curve ($x \sim t^{1/2}$). Despite evidence for non-Newtonian behaviour, the data are very well fitted by the Einstein–Roscoe Eq. (2) with the widely used value of 0.6 for ϕ_m. The apparent viscosities for bimodal distribution (50% of fines) are also plotted in Fig. 8. The data are fitted by the Einstein–Roscoe equation, but with a value of $\phi_m = 0.66$.

5. Discussion

In this section we compare our results with those obtained by other methods, and then discuss some implications focusing on volcanic processes.

5.1. Comparison of the results

Our results are consistent with others studies that used theoretical analysis, numerical simulations and laboratory measurements and show that non Newtonian behaviour initiates with the appearance of shear thinning ($n < 1$ in Eq. (8)) and yield strength near a crystal volume fraction of 0.27–0.35. These results are similar compared with others studies on magma rheology. For example a limit of 0.25 is given by Pinkerton and Norton (1995) and values of 0.22–0.285 are given by Saar et al. (2001) for cubes and spheres particles. Our results show a decrease of the n exponent from nearly 1 for mixtures with less than $\phi = 0.27$ of crystals, to $n = 0.5$ for $\phi = 0.56$. These results confirm that the threshold for solid concentration on the onset of shear thinning and the magnitude of it are general conditions of the deformation of suspensions.

The onset of yield strength occurs in our experiments for values of ϕ greater than 0.36. Saar et al. (2001) inferred in numerical

simulations a lower bound for the onset of yield strength at $\phi = 0.22$–0.28 for spherical and cubical particles. These differences can be attributed to the fact that very small yield strengths are difficult to detect in our experiments. A power law fit and the formula given by Zhou et al. (1995) fit our yield strength data better than the others (Fig. 6), but it was difficult to measure the yield strength at both high and low concentrations in our experiments. At low crystal concentrations, the final length of the flow exceeds the channel length as the fluid is still in motion. Also, the surface tension of the flow can affect the results. At the higher crystal concentrations ($\phi > 0.6$) movement was undetectable by our methods.

For liquid viscosities in the range 10–370 Pa s, the yield strength of the suspensions are not significantly affected by the suspending liquid viscosity. However, the measured yield strength for experiments with the lowest liquid viscosities (~1 Pa s) was lower than the rest of the experiments. We have not found any earlier work that address the variation of yield strength with liquid viscosity. It is not clear whether yield strength really is affected by the liquid viscosity or whether the apparent low yield strength for the ~1 Pa s liquid suspensions is an artefact of another process. We have considered the effect of low liquid viscosity on segregation of particles, greater inertia of the flow, and dissolution of particles, but none of these seem to account for the discrepancy. Segregation of particles becomes a factor after a couple of minutes in the worst scenario (big particles and low fluid viscosity), but most of the final length of the flows with low fluid viscosity is reached in a couple of seconds. A greater inertia would be reflected in the regimes observed in a distance versus time graph, which is not the case. Dissolution of particles was not observed over periods of time greater than the experiments. Further experiments are needed with a wider range of liquid viscosities in order to investigate this issue in detail.

Fig. 8 shows a very good fit of the apparent viscosity of the mixtures versus the particle concentration with the Einstein–Roscoe equation, using a value of 0.6 for ϕ_m. This value has been determined by experiments and used in magma physics and dynamics (e.g. Marsh, 1981; Pinkerton and Stevenson, 1992; Lejeune and Richet, 1995). This is a striking result, because the data are very well fitted even for values of ϕ greater than 0.3 when non-Newtonian properties appear. A possible explanation is that the values of the strain rates in the experiments are small enough that it is possible to approximate this portion of the rheological curves by a Newtonian line, as discussed by Lenk (1967), Chester et al. (1985) and Pinkerton and Stevenson (1992).

The results of the bimodal experiments are also in good agreement with previous studies with spheres. Chong et al. (1971) found that the minimum values for the relative viscosity are reached in the range of volume fractions of 0.25–0.35 of fine spherical particles, with little variation in relative viscosity for fine fractions of 0.3–0.5 of fines and rapid variations at higher or lower fine volume fractions. The observation of a higher variation of viscosity with larger particle size difference (Chong et al., 1971; Chang and Powell, 1994; Stickel and Powell, 2005) is also observed in our experiments. Our experimental system is closely analogous in terms of particle shape to magmatic suspensions, but qualitatively the rheology is similar to spheres.

Our results can be explained by changes in ϕ_m when particle size distribution is changed (Fig. 8) as discussed in previous works (e.g. Sudduth, 1993). The maximum value of ϕ_m is 0.66 and is reached with fine crystals making up half the volume of crystals. Sudduth (1993) discussed that values up to 0.86 for ϕ_m can be reached by bimodal suspensions of spherical particles with a size ratio up to 16:1. The lower ϕ_m for our experiments could be due to the different shape of the crystals used in our experiments (cubic), with a less efficient packing than spheres when randomly oriented. An alternative framework to explain our results is effective medium theory, assuming that the syrup and small crystals form the fluid phase with a viscosity calculated with the Einstein–Roscoe equation and the big crystals are the solid fraction. Fig. 7 shows a good agreement with this theory.

5.2. Comparison with other methods

Our method is inexpensive; the only materials used are a channel with a gate and a video camera to record the flow. Other advantages are: the wall slip problem for standard rotational rheometry on multiphase mixtures can be solved simply by using a roughened surface; and there is less restriction on the size of particles. In most rotational rheometers (e.g. parallel plate, cone and plate), the particle size is limited by the requirement that the particles be considerably smaller than the separation of the plates, usually measured in hundred of microns. In our setup, we can use particles sized up to a few millimetres, with the upper limit due to the sedimentation velocity, which depends on the densities of the particles and the liquid viscosity. The experimental approach opens up investigations of coarse suspensions and wide size distributions, provided that particles do not sink or float on the time scale of the experiments. Finally, the geometry of the experiments is closer to natural flow scenarios than a rotational rheometer and the method can be used to infer rheological properties from the evolution of a flow if the geometry and scaling of the experiment is setup properly (e.g., the Reynolds and Bingham number). Here we have focussed on dam break experiments in an horizontal channel, but it is straightforward to modify the analysis to consider an inclined plane or an effusion rate instead of a fixed volume. In this way the method can be applied to infer rheological properties of lava flows inside a channel, as studied by Takagi and Huppert (in press) for lavas with a Newtonian rheology.

A disadvantage of inverting dam break flows for rheology is the lack of control over the range of strain or stress applied over the mixture, which is controlled among others factors by the volume, initial height and density of the material. The volume has to be chosen carefully, a large volume can cause inertia to be dominant, and with a too small volume, the surface tension effects can be important. A partial solution to this issue is to setup the experiments in an inclined plane in order to raise the range of stresses (see Hogg and Matson, 2009). Another problem is the precision of the manual measurements compared with standard rotational rheometers; our method cannot measure very small strains. Finally, the fluid viscosity needs to be calibrated with temperature to correct for changes in room temperature.

5.3. Applications

In this section, we developed a simple 2D-model for a free-surface flow over a slope, in order to compare the velocities profiles and mean velocities using different rheologies and crystal contents.

We assume a rheology in the form of Eq. (4) and the applied stress inside the lava flow is in the form of:

$$\tau = H\rho g \sin\beta, \tag{20}$$

with H the height of the lava flow, ρ is the lava density and β is the terrain slope. The shear rate is in the form of:

$$\dot{\gamma} = \frac{du}{dz}, \tag{21}$$

where u is the flow velocity and z is the coordinate perpendicular to the surface, with the origin at the top of the flow. Combining Eqs. (4), (20) and (21) and integrating, the velocity inside the flow is given by:

$$u(z) = \begin{cases} \dfrac{Kn}{\rho g \sin\beta(n+1)}\left[\left(\dfrac{H\rho g\sin\beta-\tau_y}{K}\right)^{\frac{n+1}{n}} - \left(\dfrac{z\rho g\sin\beta-\tau_y}{K}\right)^{\frac{n+1}{n}}\right] & \text{for } h_c < z \le H \\ \dfrac{Kn}{\rho g\sin}\beta(n+1)\left(\dfrac{H\rho\sin\beta-\tau_y}{K}\right)^{\frac{n+1}{n}} & \text{for } 0 \le z \le h_c, \end{cases} \tag{22}$$

where $h_c = \frac{\tau_y}{\rho g \sin\beta}$ is the thickness of the plug region (Dragoni et al., 1986). It can be shown that the average velocity of the flow is:

$$\overline{u} = \frac{H^2 \rho g \sin\beta}{3K}\left(\frac{3n}{H^3(n+1)}\left(\frac{\rho g \sin\beta}{K}\right)^{\frac{1-n}{n}}\right) \times \left(H(H-h_c)^{\frac{n+1}{n}} - \frac{n}{2n+1}(H-h_c)^{\frac{2n+1}{n}}\right). \quad (23)$$

Note that if $n=1$ and $\tau_y=0$ the equation becomes the well known Jeffreys relationship and if $n=1$ and $\tau_y>0$ the equation is equivalent to the equation of velocity for 2D flows of Bingham materials (e.g. Dragoni et al., 1986).

We applied the model to three different cases: a) the Newtonian case, where viscosity varies with ϕ, but not with γ, following the Einstein–Roscoe equation (using $\phi_m=0.6$), b) unimodal distribution of crystals, using the Herschel–Bulkey rheology (using Eqs. (17)–(19)) and c) a bimodal distribution case, also using the Herschel–Bulkey rheology, using a $\phi_m=0.66$. We use the following values: $\rho=2500$ kg/m^3, $H=3$ m, $\beta=7°$ and $K_0=4500$ Pa s.

Fig. 9 shows the velocity profiles for the three cases, using different crystal contents ($\phi=0.3$, 0.5 and 0.55). For $\phi=0.3$ (Fig. 9a) the three cases display similar velocity profiles. For $\phi=0.5$ (Fig. 9b) the unimodal case is much slower than the bimodal and Newtonian case. For $\phi=0.55$ (Fig. 9c) the unimodal case is still slower, while the Newtonian case has higher velocities than the bimodal case due to yield strength and shear thinning effects in the latter. Fig. 9d shows that for crystal contents up to $\phi=0.4$ the mean velocities are very close for the three cases. For higher ϕ values, the Newtonian and bimodal cases velocities can be up to 10^6 higher than the unimodal case. All these results show that there are large differences on the velocities of the flow, depending on the rheology chosen, with bimodal mixtures moving much faster with higher crystal concentrations.

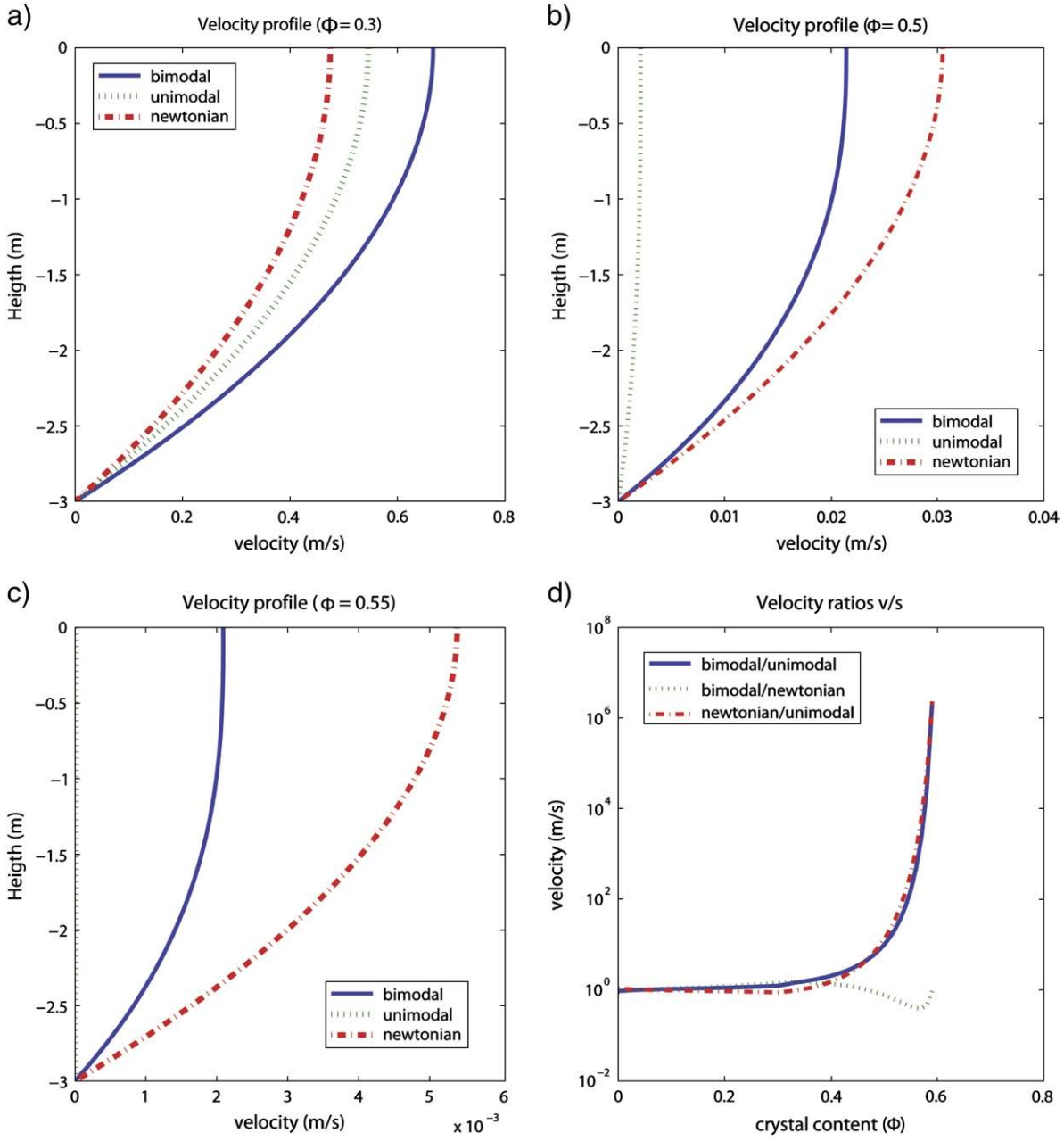

Fig. 9. Velocity profiles for lava flows with different crystal contents. Parameters used: liquid viscosity = 4500 Pa s, $\rho=2500$ kg/m^3, $H=3$ m, slope = 7°. a) $\phi=0.3$. b) $\phi=0.5$. c) $\phi=0.55$. d) Velocity ratios between the different rheological models used as a function of crystal content.

Table 1
Lava samples and flow parameters from 2002 Etna eruption.

Sample	AET-6	AET-2	AET-4
Crystal content ϕ[a]	0.45	0.61	0.54
Liquid viscosity[b] (Pa s)	4073	8317	4786
K (Pa s^n)	5.67×10^4	3.14×10^6	2.41×10^5
n	0.76	0.45	0.58
τ_y (Pa)	2.15×10^{-1}	1.89×10^2	1.89×10
Flow parameters[c]			
Flow height (m)	5	15	6
Slope (°)	7	7	12
Velocity (m/s)	1.6×10^{-1}	8.6×10^{-4}	1.1×10^{-1}
Velocity (Eq. 23)	2.6×10^{-1}	2.7×10^{-4}	4.6×10^{-2}
Apparent viscosity (Jeffreys equation)[d]	1.49×10^5	2.6×10^8	5.55×10^5
Apparent viscosity (HB eq.)[e]	1.28×10^5	6.8×10^8	1.29×10^6

[a] Crystal content was estimated by point counting (~500 points) using thin sections of the samples. Crystals were classified into phenocrysts (>1 mm) and microphenocrysts (1–0.1 mm). Microlites (<0.1 mm) were assumed that crystallized after emplacement.

[b] Liquid viscosity was calculated using the formula given by Giordano et al., 2008. Glass composition was obtained using the microprobe xx. Temperature was estimated using the glass and glass-plagioclase thermometers given by Putirka et al. (2008).

[c] Flow parameters were obtained and calculated using the reports of the eruption given by the INGV, Italy (www.ingv.it) and fieldwork done by AC.

[d] Apparent viscosity was obtained using the Jeffreys equation ($\mu_{app}=\rho g\sin\beta H^2/3V$), using the flow parameters listed in the table.

[e] Apparent viscosity was obtained with the formula $\mu_{app}=\frac{\tau}{\dot\gamma}=\frac{\tau_y}{\dot\gamma}+K\dot\gamma^{n-1}$ where $\dot\gamma$ was assumed as ~velocity/height.

5.4. Application to Etna volcano

In order to test if the parameterization we obtained in Eqs. (17)–(19) are valid for crystal-bearing lavas, we applied these equations to three samples collected from Aa basaltic lava flows from the 2002 eruption at Etna volcano (Andronico et al., 2005). The Herschel Bulkley rheological parameters were calculated from crystal contents determined from point counting on thin sections and the liquid viscosity estimated from the glass composition (Giordano et al., 2008). Then, we calculated the velocity of the flow using the 2D model described previously, and finally compared them with the actual velocities (Table 1) observed by the INGV team (www.ingv.it). Table 1 shows the calculated parameters K, n and τ_y for the three samples from Etna volcano and the calculated velocities using Eqs. (17)–(19). The computed velocities are comparable to the actual velocities, and small adjustments of the rheological and physical properties of the lava, well within the uncertainties of the measurements and estimates, could give an exact match. The calculated apparent viscosities, using the Jeffreys equation (using the height, slope and velocity of the flow) and the Herschel–Bulkley equation (using K, n and τ_y) and are also within the same order of magnitude. These results confirm the idea that the first order control on rheology of lavas is the liquid viscosity and crystal content and suggest that the combination of syrup plus sugar crystals is a good analogue of crystal-bearing lavas and the parameterization of Herschel–Bulkley equation (Eqs. (17)–(19)) can adequately describe the resulting rheology of crystal-bearing lavas.

6. Conclusions

In this work, we have demonstrated an inexpensive and easy method to carry out measurements on the rheology of suspensions. We assumed a Herschel–Bulkley rheology, and the determination of the parameters K, n and τ_y in Eq. (4) are in a good agreement with other investigations using other methods. Our experiments show a non-Newtonian behaviour for concentrations greater than ~30% of crystals, with a decrease of the n exponent from 1 to ~0.5 for $\phi\sim0.6$ and the appearance of a yield strength. The experiments with bimodal suspensions show a dramatic drop in the apparent viscosity compared with the unimodal suspensions with the same total concentration, with differences greater than 1 order of magnitude for $\phi>0.6$. These changes can be modelled assuming that the liquid and small particles constitute the fluid phase and the larger particles are the solid phase. Alternatively, it can be explained with changes in the maximum packing fraction. Changes of size distribution also affect the rheological threshold when the Einstein–Roscoe equation can no longer predict the apparent viscosity of the mixture. The results of the yield strength values are not totally clear, and further studies are required to determine if liquid viscosity affects the results and to explain the differences between yield strengths measured with analogue materials and the ones found on lavas flows on the field.

The differences in the rheology showed by suspensions with different size distributions have important implications for the dynamics of magma flows. In particular, the simplified 2-D model for an inclined flow using a Herschel–Bulkley rheology shows strong differences in flow profile and velocity, with higher velocities in lavas with polymodal crystal size distribution. We applied the equations for the parameters K, τ_y and n to lavas from Etna volcano and the calculated velocities are in very good agreement with the actual velocities, suggesting that our results can be applied to calculate the rheology of real crystal-bearing lavas. Our results may also have implications regarding the eruptibility of highly crystalline magmas. Polymodal suspensions have a higher limit of crystal content for viscous behaviour (given by the maximum packing fraction) and this can explain why some very crystal-rich magmas (e.g. Soufriere-Hills volcano, Sparks et al., 2000) are able to erupt.

Acknowledgements

AC thanks the help of the INGV, Catania, Italy, during the fieldwork on Etna volcano and the financial support given by Government of Chile through the Presidente de la Republica scholarship. ACR thanks the Royal Society of a University Research Fellowship. RSJS thanks the support of a European Research Council Advanced Grant. The authors thank Megan Arnold for helping with some of the experiments presented here and Katie Hauff for some preliminary experimental results. The comments of R. C. Kerr and an anonymous reviewer helped to improve the paper.

Appendix A. Supplementary data

Supplementary data associated with this article can be found, in the online version, at doi:10.1016/j.epsl.2010.06.051.

References

Andronico, D., Branca, S., Calvari, S., Burton, M.R., Caltabiano, T., Corsaro, R.A., Del Carlo, P., Garfì, G., Lodato, L., Miraglia, L., Murè, F., Neri, M., Pecora, E., Pompilio, M., Salerno, G., Spampinato, L., 2005. A multi-disciplinary study of the 2002–03 Etna eruption: insights for a complex plumbing system. Bull. Volcanol. 67, 314–330.
Balmforth, N.J., Craster, R.V., 2000. Dynamics of cooling domes of viscoplastic fluid. J. Fluid Mech. 422, 225–248.
Balmforth, N.J., Craster, R.V., Perona, P., Rust, A.C., Sassi, R., 2007. Viscoplastic dam breaks and the Bostwick consistometer. J. Non-Newtonian Fluid Mech. 142 (1–3), 63–78.
Barnes, H.A., 1995. A review of the slip (wall depletion) of polymer solutions, emulsions and particle suspensions in viscometers; its cause, character and cure. J. Non-Newtonian Fluid Mech. 56, 221–251.
Barnes, H.A., 1999. The yield stress—a review or πανταρει-everything flows? J. Non-Newtonian Fluid Mech. 81, 133–178.
Caricchi, L., Burlini, L., Ulmer, P., Gerya, T., Vassalli, M., Papale, P., 2007. Non-Newtonian rheology of crystal-bearing magmas and implications for magma ascent dynamics. Earth Planet Sci. Lett. 264, 402–419.
Chang, C., Powell, R.L., 1993. Dynamic simulation of bimodal suspensions of hydrodynamically interacting spherical particles. J. Fluid Mech. 253, 173–209.
Chang, C., Powell, R.L., 1994. Effect of particle size distributions on the rheology of concentrated bimodal suspensions. J. Rheol. 38, 85–98.
Chester, D.K., Duncan, A.M., Guest, J.E., Kilburn, C.R.J., 1985. Mount Etna: The Anatomy of a Volcano. Stanford University press. 404 pp.
Chong, J.S., Christiansen, E.B., Baer, A.D., 1971. Rheology of concentrated suspensions. J. Appl. Polym. Sci. 15, 2007–2021.

Costa, A., 2005. Viscosity of high crystal content melts: dependence on solid fraction. Geophys. Res. Lett. 32. doi:10.1029/2005GL024303.
Costa, A., Caricchi, L., Bagdassarov, N., 2009. A model for the rheology of particle-bearing suspensions and partially molten rocks. Geochem. Geophys. Geosyst. G3 10, N3.
Dingwell, D.B., 1996. Volcanic dilemma: flow or blow? Science 273, 1054–1055.
Dragoni, M., Tallarico, A., 1994. The effect of crystallisation on the rheology and dynamics of lava flows. J. Volcanol. Geoth. Res. 59, 241–252.
Dragoni, M., Bonafede, M., Boschi, E., 1986. Downslope flow models of a Bingham liquid: implications for lava flows. J. Volcanol. Geoth. Res. 30, 305–325.
Dragoni, M., Borsari, I., Tallarico, A., 2005. A model for the shape of lava flow fronts. J. Geophys. Res. 110, B09203.
Einstein, A., 1906. Eine neue Bestimmung der Molekuldimensionen. Ann. Phys. 19, 289–306.
Gay, E.C., Nelson, P.A., Armstrong, W.P., 1969. Flow properties of suspensions with high solid concentrations. AIChE J. 15, 815–822.
Giordano, D., Russell, J.K., Dingwell, D.B., 2008. Viscosity of magmatic liquids: a model. Earth Planet. Sci. Lett. 271, 123–134.
Harris, A.J.L., Rowland, S.K., 2001. FLOWGO: a kinematic thermo-rheological model for lava flowing in a channel. Bull. Volcanol. 63, 20–44.
Herschel, W.H., Bulkley, R., 1926. Konsistenzmessungen von Gummi-Benzol-Lösungen. Kolloid Z. 39, 291–300.
Hogg, A.J., Matson, G.P., 2009. Slumps of viscoplastic fluids on slopes. J. Non-Newtonian Fluid Mech. 158 (1–3), 101–112.
Hoover, S., Cashman, K.V., Manga, M., 2001. The yield strength of subliquidus basalts: experimental results. J. Volcanol. Geoth. Res. 107, 1–18.
Hulme, G., 1974. The interpretation of lava flow morphology. Geophys. J. R. Astr. Soc. 39, 361–383.
Huppert, H.E., 1982a. The propagation of two-dimensional and axisymmetric viscous gravity currents over a rigid horizontal surface. J. Fluid Mech. 121, 43–58.
Huppert, H.E., 1982b. Flow and instability of a viscous current down a slope. Nature 300, 427–429.
Huppert, H.E., Sparks, R.S.J., 1988. The generation of granitic magmas by intrusion of basalt into continental crust. J. Petrol. 29, 599–624.
Huppert, H.E., Shepherd, J.B., Sigurdsson, H., Sparks, R.S.J., 1982. On lava dome growth, with application to the 1979 lava extrusion of the Soufrière of St. Vincent. J. Volcanol. Geoth. Res. 14, 199–222.
Ishihara, K., Iguchi, M., Kamo, K., 1990. Numerical simulation of lava flows on some volcanoes in Japan. In: Fink, J.H. (Ed.), Lava Flows and Domes; Emplacement Mechanisms and Hazard Implications. Springer, Berlin, pp. 174–207.
Kerr, R., Lister, J., 1991. The effects of shape on crystal settling and on the rheology of magmas. J. Geol. 99, 457–467.
Kerr, R.C., Lyman, A.W., 2007. Importance of surface crust strength during the flow of the 1988–1990 andesite lava of Lonquimay Volcano, Chile. J. Geophys. Res. 112, B03209. doi:10.1029/2006JB004522.
Krieger, I.M., Dougherty, T.J., 1959. A mechanism for non-Newtonian flow in suspensions of rigid spheres. Trans. Soc. Rheol. 3, 137–152.
Lavallée, Y., Hess, K.-U., Cordonnier, B., Dingwell, D.B., 2007. Non-Newtonian rheological law for highly crystalline dome lavas. Geology 35, 843–846.
Lejeune, A., Richet, P., 1995. Rheology of crystal-bearing silicate melts: an experimental study at high viscosity. J. Geophys. Res. 100, 4215–4229.
Lenk, R.S., 1967. A generalized flow theory. J. Appl. Polym. Sci. 11, 1033–1042.
Lyman, A.W., Kerr, R.C., 2006. Effect of surface solidification on the emplacement of lava flows on a slope. J. Geophys. Res. 111, B05206.
Lyman, A.W., Koenig, E., Kerr, R.C., 2004. Predicting yield strengths and effusion rates of lava domes from morphology and underlying topography. J. Volcanol. Geoth. Res. 129, 125–138.
Lyman, A.W., Kerr, R.C., Griffiths, R.W., 2005. Effects of internal rheology and surface cooling on the emplacement of lava flows. J. Geophys. Res. 110, B08207.
Marsh, B., 1981. On the crystallinity, probability of occurrence, and rheology of lava and magma. Contrib. Mineral. Petrol. 78, 85–98.
Mcbirney, A.R., Murase, T., 1984. Rheological properties of magmas. Annu. Rev. Earth Planet. Sci. 12, 337–357.
Melnik, O., Sparks, R.S.J., 1999. Nonlinear dynamics of lava dome extrusion. Nature 40, 37–41.
Nye, J., 1952. The mechanics of glacier flow. J. Glaciol. 2, 82–93.
Papale, P., 2001. The dynamics of magma flow in volcanic conduits with variable fragmentation efficiency and non-equilibrium pumice degassing. J. Geophys. Res. 106, 11043–11065.
Papale, P., Neri, A., Macedonio, G., 1998. The role of magma composition and water content in explosive eruptions. 1. Conduit ascent dynamics. J. Volcanol. Geoth. Res. 87, 75–93.
Petford, N., 2003. Rheology of granitic magmas during ascent and emplacement. Annu. Rev. Earth Planet. Sci. 31, 399–427.
Petford, N., Koenders, M.A., 1998. Granular flow and viscous fluctuations in low Bagnold number granitic magmas. J. Geol. Soc. Lond. 155, 873–881.
Pinkerton, H., Norton, G.E., 1995. Rheological properties of basaltic lavas at sub-liquidus temperatures: laboratory and field measurements on lavas from Mount Etna. J. Volcanol. Geoth. Res. 68, 307–323.
Pinkerton, H., Stevenson, R.J., 1992. Methods of determining the theological properties of lavas from their physicochemical properties. J. Volcanol. Geoth. Res. 53, 47–66.
Putirka, K., 2008. Thermometers and barometers for volcanic systems. Reviews in Mineralogy & Geochemistry 69, 61–120.
Robson, G.R., 1967. Thickness of Etnean lavas. Nature 216, 251–252.
Roscoe, R., 1952. The viscosity of suspensions of rigid spheres. Br. J. Appl. Phys. 3, 267.
Ryerson, F.J., Weed, H.C., Piwinskii, A.J., 1988. Rheology of subliquidus magmas 1. Picritic compositions. J. Geophys. Res. 93, 3421–3436.
Saar, M., Manga, M., Cashman, K.V., Fremouw, S., 2001. Numerical models of the onset of yield strength in crystal-melt suspensions. Earth Planet. Sci. Lett. 187, 367–379.
Shaw, H.R., 1969. Rheology of basalt in the melting range. J. Petrol. 10, 510–535.
Soule, S.A., Cashman, K.V., 2005. The shear rate dependence of the pahoehoe-to-aa transition: analog experiments. Geology 33, 361–364.
Sparks, R.S.J., 2003. Forecasting volcanic eruptions. Earth Planet. Sci. Lett. 210, 1–15.
Sparks, R.S.J., Pinkerton, H., Hulme, G., 1976. Classification and formation lava levées on Mount Etna, Sicily. Geology 4, 269–271.
Sparks, R.S.J., Murphy, M.D., Lejeune, A.M., Watts, R.B., Barclay, J., Young, S.R., 2000. Control on the emplacement of the andesite lava dome of the Soufriere Hills Volcano by degassing-induced crystallization. Terra Nova 12, 14–20.
Stasiuk, M.V., Jaupart, C., Sparks, R.S.J., 1993. Influence of cooling on lava flow dynamics. Geology 21, 335–338.
Stickel, J.J., Powell, R.L., 2005. Fluid mechanics and rheology of dense suspensions. Annu. Rev. Fluid Mech. 37, 129–149.
Sudduth, R.D., 1993. A new method to predict the maximum packing fraction and the viscosity of solutions with a size distribution of suspended particles II. J. Appl. Polym. Sci. 48, 37–55.
Takagi, D., Huppert, H., 2010. Initial advance of long lava flows in open channels. J. Volcanol. Geoth. Res. 195, 121–126.
Walker, G.P.L., 1967. Thickness and viscosity of Etnean lavas. Nature 213, 484–485.
Zhou, J.Z.Q., Fang, T., Luo, G., Ulherr, P.H.T., 1995. Yield stress and maximum packing fraction of concentrated suspensions. Rheol. Acta 34, 544–561.